Journal of Electroanalytical Chemistry 914 (2022) 116303

Contents lists available at ScienceDirect

Journal of Electroanalytical Chemistry

journal homepage: www.elsevier.com/locate/jelechem

Self-assembled monolayers of O-(2-Mercaptoethyl)-O′-methyl-hexa(ethylene glycol) (EG7-SAM) on gold electrodes. Effects of the nature of solution/electrolyte on formation and electron transfer blocking characteristics

Miriam Chávez, Guadalupe Sánchez-Obrero, Rafael Madueño, José Manuel Sevilla, Manuel Blázquez, Teresa Pineda *

Department of Physical Chemistry and Applied Thermodynamics, Institute of Fine Chemistry and Nanochemistry, University of Cordoba, Campus Rabanales, Ed. Marie Curie 2ª Planta, E-14014 Córdoba, Spain

ARTICLE INFO

Keywords:
Polyethylene glycol
Self-assembled monolayer
Gold electrode
Cyclic voltammetry
Electrochemical impedance spectroscopy
Contact angle measurements

ABSTRACT

The self-assembly of O-(2-Mercaptoethyl)-O'-methyl-hexa(ethylene glycol) (EG7) on gold substrates produces monolayers whose structure should depend primarily on the solvents used for their formation. Although this should be also the case for any self-assembled monolayer (SAM) system, the presence of oxygen atoms in the EG7 chains brings about specific interactions with the solvent molecules other than just the van der Waals interactions taking place with alkanethiols. In this work we investigate the effects of the nature of the solutions for EG7-SAM formation in the reductive desorption processes using gold substrates either polycrystalline or single crystal electrodes. The patterns obtained in polycrystalline substrates are compared to the peaks observed at gold single crystal electrodes and it has been found that the main peaks correspond to the molecules desorbed from the different gold facets contained in the polycrystalline substrate. These single peaks are in fact composed of at least two contributions that can be explained as the presence of domains where the EG7 molecules are organized with different orientations, giving place to intermolecular interactions of different magnitude. The blocking properties of these films are strongly determined by the nature of the electrolyte used for the analysis and not by the solvent used in their formation. Although no experimental evidence of the specific interaction and/or retention inside the film of Na^+ or phosphate or both ions is obtained, a specific effect that accounts for an electron transfer rate constant of an order of magnitude lower than the obtained with other electrolytes is observed. These results can contribute to increase the understanding of the relationship between the EG7-SAMs structure and functionalities.

1. Introduction

The construction of multifunctional interfaces with tailored properties is an important research topic that is nowadays attracting the attention in the field of biocompatible and functional materials. Self-assembled monolayers (SAMs) constitute one of the most utilized strategies to create functional interfaces due to the easy preparation and the huge number of molecules available to assemble on different solid surfaces [1,2].

The dynamic equilibrium governing the adsorption of thiols on solid surfaces is influenced by the solvent-substrate and the solvent-adsorbate interactions, and the rates of formation depend on the magnitude of these interactions that can be tuned by the solvent-adsorbate interaction strength [1]. In this sense, the use of polar solvents that present low solubility for alkanethiols can contribute to their assembly at the substrate surface [3,4]. Results obtained by scanning tunneling microscopy have shown that solvents of high polarity improve the quality of alkanethiol SAMs due to the strong hydrophobic interactions between the nonpolar hydrophobic tails, whereas the low polarity solvents can disturb the tight packing of the monolayer [5]. The presence of surfactants of low critical micellar concentration in water solutions has demonstrated to contribute to the formation of highly compact alkanethiol SAMs by providing hydrophobic domains that solubilize the alkane tails and facilitate their delivery to the substrate surface [6–13].

* Corresponding author.
E-mail address: tpineda@uco.es (T. Pineda).

https://doi.org/10.1016/j.jelechem.2022.116303
Received 27 December 2021; Received in revised form 31 March 2022; Accepted 8 April 2022
Available online 11 April 2022

Oligo-ethylene glycol (OEG)-terminated alkanethiols have been widely used to form SAMs taking the advantage of the long alkane arm that directs the organization of the molecules resulting in compact layers that expose the OEG-terminal to the medium. The OEG portion, under these conditions, can adopt either a helical or an all-trans conformation depending on factors such as the type of substrate [14,15], the surface coverage [16,17], the number of EG units [15,17] and the solvent [18]. These SAMs have demonstrated to minimize the unspecific adsorption of proteins and inhibit cell attachment [14,15,19,20] depending on the amount of water associated with the OEG chains that ultimately depends on its conformation [21,22].

Most of the surfaces modified with ethylene glycol used in the actual applications employ mercapto-poly-ethylene glycol (EGn) molecules that lack the alkane arm, and the organization of these layers results obviously different and dependent on other parameters such as temperature or the presence of different salts in the formation solution [23–26]. One of the shortest EGn chains available is O-(2-Mercaptoethyl)-O'-methyl-hexa(ethylene glycol) (EG7) and can be used as a model for the characterization of the EGn-SAMs. We have recently reported that the EG7-SAM formed from an EG7 ethanolic solution acquires the best structural performance at a modification time of 1 h. Under these conditions, the cyclic voltammograms for the reductive desorption process obtained from a polyoriented (PO) gold electrode shows a set of discrete peaks that cannot be only explained on the basis of the desorption from different defined gold facets present in the surface, but the existence of different degrees of intermolecular interactions need to be introduced in the scene [27]. Dealing with the use of EGn layers on electrochemical biosensors to avoid the nonspecific adsorption phenomenon and the drawback of inhibition of the heterogeneous electron transfer kinetics, Doneux et al. [28,29] studied the electrochemical performance of the EG7-SAM using different outer sphere redox probes such as $[Fe(CN)_6]^{3-/4-}$, $[Ru(NH_3)_6]^{3+/2+}$, $Fc(MeOH)^{2+/0}$, and $[IrCl_6]^{2-/3-}$, to investigate the monolayer barrier properties. They found that the EG7-SAM behaves as a low impedance film [30] with all the assayed redox probes except for the $[Fe(CN)_6]^{3-/4-}$ system. They interpreted the high electron transfer inhibition in terms of the hydration properties of both the monolayer and the electroactive anions. In an earlier study by Vanderah et al. [31] on the influence of the solvent used for the SAM formation on the structure of the EG7-SAM, as characterized by ellipsometry, infrared reflection–absorption spectroscopy (IRRAS) and electrochemical impedance spectroscopy (EIS), they choose within a nonhydroxylic solvent as THF, a hydroxylic EtOH and also select an ethanol/water mixture, $EtOH_{95}$, to discern the effect of the presence of water in the formation solution. The best performance was found for the layer produced from the $EtOH_{95}$ solution. Moreover, whereas the EG7-SAMs formed from EtOH and $EtOH_{95}$ showed the same thickness, that from THF solvent present a variable value, indicating a more irregular structure. Similarly, the layer formed from $EtOH_{95}$ behaves as an almost perfect capacitor but for those from EtOH and THF, the heterogeneity obliges to introduce the constant phase element to account for the deviation of that ideal behavior. Finally, infrared spectroscopy revealed a highly organized structure for both layers formed in ethanol and a less ordered film when formed in THF.

Pioneering works on alkanethiol SAMs reductive desorption processes have already established the type of information that can be obtained in relation to SAMs stability and organization [32–38], and now it is widely accepted that the process can be considered as a solvent substitution reaction,

$$RS_{(SAM,Au(hkl))} + xH_2O_{(aq)} + ne^-_{(Au(hkl))} \rightleftharpoons RS^-_{(aq)} + xH_2O_{(surf,\ Au(hkl))} \quad (1)$$

that involves the different energetic contributions such as substrate-adsorbate, intermolecular lateral, substrate-SAM-solvent, free surfactant-solvent and substrate-solvent interactions [38–41].

In this context and taking the EG7-SAM as a model for the PEGylated surfaces, we have explored its electrochemical behavior by going deeper into the reductive desorption processes by using different gold substrates. To this end, the EG7-SAMs are formed in different media, from these already described by Vanderah et al. [31] to the sodium phosphate aqueous solution. Moreover, these EG7-SAMs are also characterized by electrochemical impedance spectroscopy in different neutral media to find out the influence of the electrolyte in the electrochemical response of the $[Fe(CN)_6]^{3-/4}$ redox probe. Whereas the solvent used for the formation of the SAM influences the structure as observed in the reductive desorption signatures, the blocking ability against the redox probe is not affected. In contrast, the electrolyte solution used for this analysis tunes the electrochemical response influencing the apparent electron transfer rate constant values.

2. Experimental section

2.1. Chemicals

O-(2-Mercaptoethyl)-O′-methyl-hexa(ethylene glycol) (EG7), Potassium hexaferricyanide and potassium hexaferrocyanide ($[Fe(CN)_6]^{3-/4-}$), were purchased from Aldrich-Sigma (purity ≥ 99%). The rest of the reagents were from Merck analytical grade. All the aqueous solutions were prepared with deionized ultrapure water produced by Millipore system.

2.2. Experimental methods

Electrochemical experiments were performed on an Autolab (Ecochemie model Pgstat30) instrument attached to a PC with proper software (GPES and FRA) for the total control of the experiments and data acquisition. A conventional three electrode cell comprising a platinum coil as counter electrode, a 50 mM KCl calomel (CE 50 mM) as reference electrode and either a poly-oriented (PO gold) or single crystals gold (Au(1 1 1), Au(1 0 0) and Au(1 1 0)), as the working electrodes, were used. The PO gold electrode was a homemade sphere obtained by melting a gold wire up to reach a diameter of approximately 2 mm and attached to the gold wire that serves as electrode connection. The single crystals were 3 mm diameter and 2 mm thick cylinders from Metal Crystals & Oxides LTD, with a polished side. A gold wire, mounted at the rear end, allowed easier handling of the crystal. Before each electrochemical measurement, the electrodes were annealed in a natural gas flame to a light-red melt for about 20 s and, after a short period of cooling in air, quenched in ultrapure water. The electrodes were then transferred into the electrochemical cell with a droplet of water adhering to it to prevent contamination and were contacted with the solution by the meniscus method, under potential controlled conditions. Each surface of the single crystals used in this study showed the well-known characteristic voltammograms in 0.01 M $HClO_4$ solutions. The real area of the gold electrodes were determined from the charge involved in the gold oxide reduction peaks obtained under these conditions ($A_{(PO\ gold)}$ = 0.24 cm^2; $A_{(Au(1\,1\,1)}$ = 0.09 cm^2; $A_{(Au(1\,0\,0)}$ = 0.09 cm^2; $A_{(Au(1\,1\,0)}$ = 0.10 cm^2).

For electrode modification, the gold electrodes were immersed in the EG7 solutions (either of pure ethanol (EtOH) or 95 % ethanol ($EtOH_{95}$) or tetrahydrofuran (THF) or sodium phosphate (NaPi) 1 M) for a modification time of 1 h (Scheme 1). After extensive washing with water or blank electrolyte, they were transferred to the electrochemical cell, to carried out the cyclic voltammetry or electrochemical impedance spectroscopy experiment.

The cyclic voltammograms for the reductive desorption processes were recorded in KOH 0.1 M solutions and these for the evaluation of the electron transfer in aqueous solutions were of sodium phosphate (NaPi) 0. 1 M at pH 7.4, KNO_3 0.1 M and KCl 0.1 M in the presence of 1 mM $[Fe(CN)_6]^{3-/4-}$. The electrochemical impedance spectroscopy

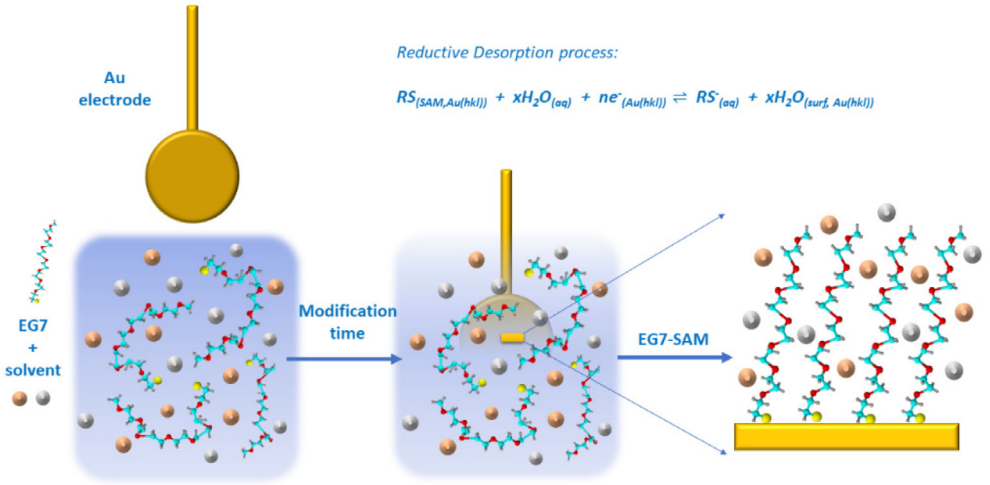

Scheme 1. Formation of EG7-SAM on an Au electrode.

measurements were obtained at the midpoint potential of the cyclic voltammogram registered for the naked electrode (at 0.08 V), using an amplitude rms of 10 mV and a frequency interval from 0.1 to 10000 Hz.

Contact Angle measurements were conducted by using an Optical Tensiometer Theta T200 device (Attension, Biolin Scientific) equipped with a high-speed camera (420 fps). The CA of the formed SAMs was measured in sessile drop method. The experiments were performed at room temperature and at open atmosphere. The results are given as an average of six measurements.

3. Results and discussion

3.1. Reductive desorption of EG7-SAMs formed in different media

We have previously reported results on the characterization of a compact EG7-SAM formed from EtOH solution by using electrochemical and spectroscopic techniques [27]. In particular, the results of the reductive desorption process monitored by cyclic voltammetry show a set of peaks with a shape that depends on the modification time. In a first approximation, the peaks are ascribed to the desorption of portions of monolayer from the different facets existing in the PO gold whose peak potentials follow the trend of the potential of zero charge (*pzc*) of these naked facets. However, there are some details in the cyclic voltammograms that cannot be explained only on this basis. To get more insight into this system, we first studied the reductive desorption process of the EG7-SAM formed in different solvents on a PO gold electrode. Considering previous results on the organization of this SAM formed from EtOH, $EtOH_{95}$ and THF, characterized by electrochemical impedance and infrared spectroscopies [31], and that formed from a 1 M NaPi solution analyzed by cyclic voltammetry [28,29], the reductive desorption processes of the SAMs formed under the same experimental conditions are here examined.

Fig. 1 shows the cyclic voltammograms for these reductive desorption processes that show that, although all of them share the multipeak shape, they differ in the shape and in the potentials of the individual peaks. Moreover, there is no clear trend on the peak potential variations. While the SAM formed from EtOH, $EtOH_{95}$ and THF present a similar pattern with four peaks, that formed from 1 M NaPi aqueous solution shows only three peaks that are displaced 50 mV in the positive direction. However, the charge densities involved in the overall reductive desorption peaks are almost equal and independent on the nature of the solvent used for its formation.

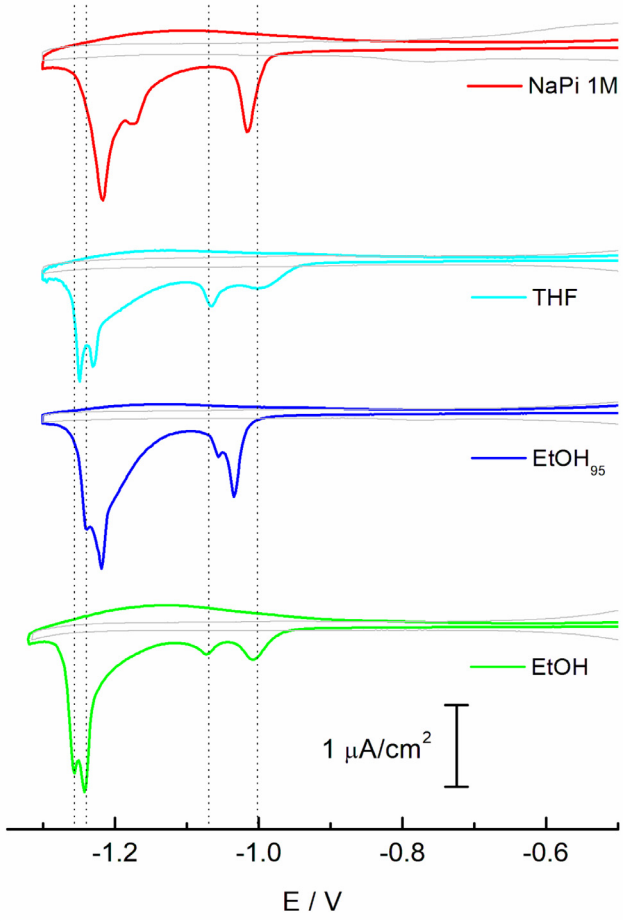

Fig. 1. Cyclic voltammograms for the reductive desorption process of the EG7-SAM on PO gold electrodes in KOH 0.1 M solution. The grey line represents the blank profiles obtained in the same solution. v = 20 mV/s. The SAMs have been formed in different solvents as labeled, at a modification time of 1 h.

Pioneering works using single crystal gold electrodes to ascribe the multipeak voltammetry obtained at polycrystalline gold electrodes tried to explain the differences in peak potential as different energetics of the Au-S bond on the various single crystal gold facets. Thus, the dif-

ferences in potential were correlated to the potential of zero charge of the naked surfaces [33,37]. In this context, many systems have been analyzed and the peaks have been assigned to monolayer domains desorbed from Au(1 1 1), Au(1 0 0) and Au(1 1 0) facets [36,38,42–44]. Moreover, the type of sulfur adsorption sites depending on the ordering of the surface gold atoms in the facet, either reconstructed or unreconstructed, was also entered in the discussion, indicating that the cohesive interactions between neighboring adsorbates would vary with these different binding sites thus influencing the packing density [45]. Recently, the classical way of considering the peak potential of the reductive desorption as a measure of the Au-S bond energy was reinforced by considering the different contributions included in the energy change between the initial and final states of the reductive desorption reaction represented by reaction (1). This equation is a substitution reaction between the adsorbate and the solvent [38,39]. Thus, the adsorbate–surface interaction involves the Au-S bond that should be directly correlated with the crystallographic orientation. However, the different interactions of the adsorbates whether in the adsorbed state or free in solution would affect the energetics of desorption. Studies by Cometto et al. [41,46] on the electrochemical stability of alkanethiol SAMs of different chain length on planar and curved surfaces compare the position of the reductive desorption peaks obtained on Au(1 1 1) and Au(1 0 0) single crystal electrodes. They found that the differences in the reductive desorption potentials in these substrates increase with the alkanethiol chain length, suggesting a preferential adsorption of the SAMs on the Au(1 0 0). Analyzing the different contributions of the interactions taking place in the reductive desorption process, they found that the shift in the potential for a given SAM formed on different surfaces depends on the substrate-adsorbate interactions that are determined by the energy of the Au-S bond, the adsorbate–adsorbate interaction determined by the lateral interactions mainly consisting of vdW forces, the different thiol-solvent interactions in the adsorbed state that depends on the *pzc* of the SAM, the solvation energy of the free alkanethiols and the solvent-substrate interactions that again depend on the *pzc* of the naked gold surfaces.

To get more insight into the nature of the peaks obtained for the desorption of monolayer domains from different gold facets and correlate them for the SAMs formed under different solvent conditions, we have carried out a study of the formation of EG7-SAM in the different media described above, and its reductive desorption processes using Au(1 1 1), Au(1 0 0) and Au(1 1 0) single crystal electrodes.

Starting with the EG7-SAM formed in EtOH, we obtain a single peak at −0.99 V (peak 1) on the Au(1 1 1) surface that is very close to the first peak in the PO gold as already reported [27]. The process on Au(1 0 0) and Au(1 1 0) show broad peaks at −1.21 and −1.20 V (peak 3 and 4), respectively (Fig. 2). Besides these, a small peak at −0.985 V is seen in the Au(1 0 0) surface at potentials close to peak 1 on the Au(1 1 1) facet. A small peak at −1.07 V (peak 2) is also obtained at the Au(1 1 0) that is also coincident with the second peak on the PO gold surface. It is interesting to note that the peaks 3 and 4 are shifted to higher potentials (~40 mV) in respect to these corresponding in the PO gold electrode. These features are also observed in the cyclic voltammograms recorded for the EG7-SAM formed in THF (Fig. 2).

The trend obtained for the EG7-SAM formed in NaPi presents important differences. First, only three peaks appear in the cyclic voltammogram for the PO gold. The first one is sharp and is comprised in the potential interval where the main peak in Au(1 1 1) and the smaller peaks in Au(1 0 0) and Au(1 1 0) appear (peaks 1 and 2). It must be noted that, in contrast to what happens in the PO gold, the main peak in Au(1 1 1) is broad and seems to be formed by two overlapped peaks. Second, the lower potential peaks in PO gold are almost coincident with the mean peaks at (1 0 0) and (1 1 0) surfaces. Finally, the EG7-SAM formed in $EtOH_{95}$ presents an Au(1 1 1) peak that occurs at 85 mV higher potential that the first peak in the PO gold surface. The rest of the peaks in the single crystals lay very close to those of the PO gold electrode.

Fig. 3 shows the above commented peak potentials for the PO and the single crystal electrodes and, as it can be observed, the potentials for each peak are within the intervals of 55 to 80 mV, indicating that they can represent similar energetic situations.

As observed in Fig. 2, most of the main peaks obtained in the reductive desorption process at single crystal electrodes seems to contain more than one contribution. To get more information about the origin

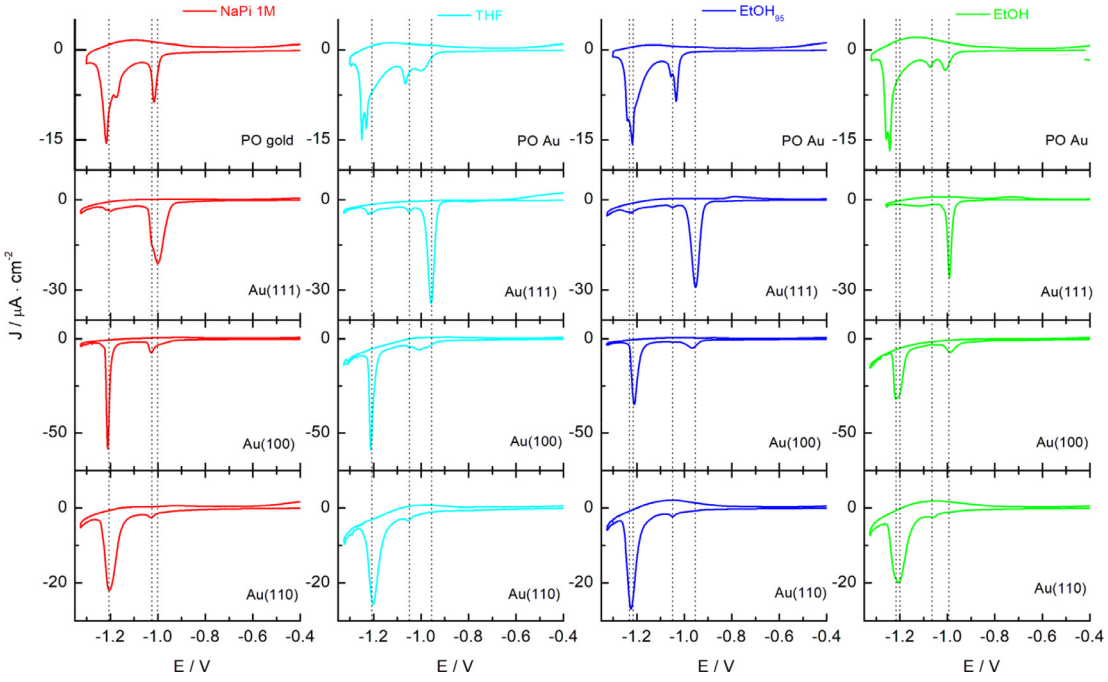

Fig. 2. Cyclic voltammograms for the reductive desorption processes of the EG7-SAMs on PO gold and Au(1 1 1), Au(1 0 0) and Au(1 1 0) single crystal electrodes in KOH 0.1 M solution. v = 20 mV/s. The SAMs have been formed in different solvents as labeled, at a modification time of 1 h.

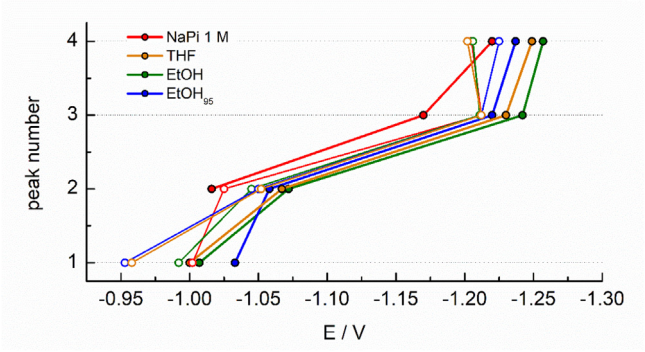

Fig. 3. Potential values for the different peaks observed in the reductive desorption process of EG7-SAM on a PO (solid circles) and single crystal (empty circles) gold electrodes. While the PO gold electrode peaks (1, 2, 3 and 4) correspond to these observed in the cyclic voltammograms, these for the single crystals are: 1, main peak in Au(1 1 1); 2, small first peak in Au(1 1 0); 3, main peak in Au(1 0 0); 4, main peak in Au(1 1 0).

of the peaks, and after eliminating the background currents, we have carried out a deconvolution of these peaks, by using Lorentzian curves (Figure S1). We have used three contributions to fit the cyclic voltammograms that are named as peak 1, 2 and 3 in Fig. 4, where the peak potential, the half width, and the percentage of area for each component are represented. The cyclic voltammogram recorded for the EG7-SAM formed in NaPi in a Au(1 1 1) single crystal, can be fitted with two peaks at −0.99 and −1.02 V with a half width of around 30 mV and a charge density that supposes 53 and 34 % of the total charge, and a third peak at −1.19 V of very low charge (~12%) that should correspond to molecules desorbed from step or defect sites on the (1 1 1) facet. This double contribution observed in the single crystal and absent in the peak obtained at the same potentials in the PO surface, must be assigned to monolayer domains with different intermolecular interactions that can be produced when larger terraces exist on the Au(1 1 1) single crystal surface as it should be the case, in comparison to the PO gold surface. In the case of EtOH as solvent, two contributions are also present with similar half width but being the second contribution of lower significance. The cyclic voltammograms of the SAMs built in $EtOH_{95}$ or THF also show this second type of contribution, but both are of very low charge density in comparison to the first one.

The curves obtained with Au(1 0 0) show a first peak between −1.025 V and −0.97 V that are very close to the second contribution of the (1 1 1) facet and involve a charge density lower that 20 % of the total amount measured. The main peak, although very sharp requires the introduction of two signals that are also of a very low width (half width of less than 20 mV), and these are of the same magnitude in the case of the SAMs prepared in EtOH and THF and of a ratio 60:30 in the SAMs prepared in NaPi or $EtOH_{95}$. It can be thought that the first peak observed in the (1 0 0) facet should have an origin on either, a small portion of reconstructed hexagonal surface or some stepped sites that would show a similar energetic than the (1 1 1) domain that we obtain as a second contribution in that facet. The presence of two domains with different molecular interactions on the (1 0 0) facet could explain the presence of the double contribution in the main peak. The fact that the SAMs formed in NaPi and $EtOH_{95}$ present a major contribution in the higher potential peak that is assigned as less energetic, can be ascribed to the effect of water molecules on the organization of the layer. In the case of EtOH and THF, the absence of water in the formation solution avoids this and the adsorbed molecules should share conformation.

In the deconvolution of the reductive desorption with Au(1 1 0), besides the first small peak at −1.045 V that coincides with the more negative potential region where the (1 1 1) peaks are obtained, a broad signal at more negative potential is observed for all the SAMs independent on the solvent used in the formation solution. The peak is also deconvoluted introducing two contributions of similar widths and area ratio.

The presence of multi-wave voltammetry in the reductive desorption peaks of long alkanethiol SAMs has been observed in Au(1 1 1) sin-

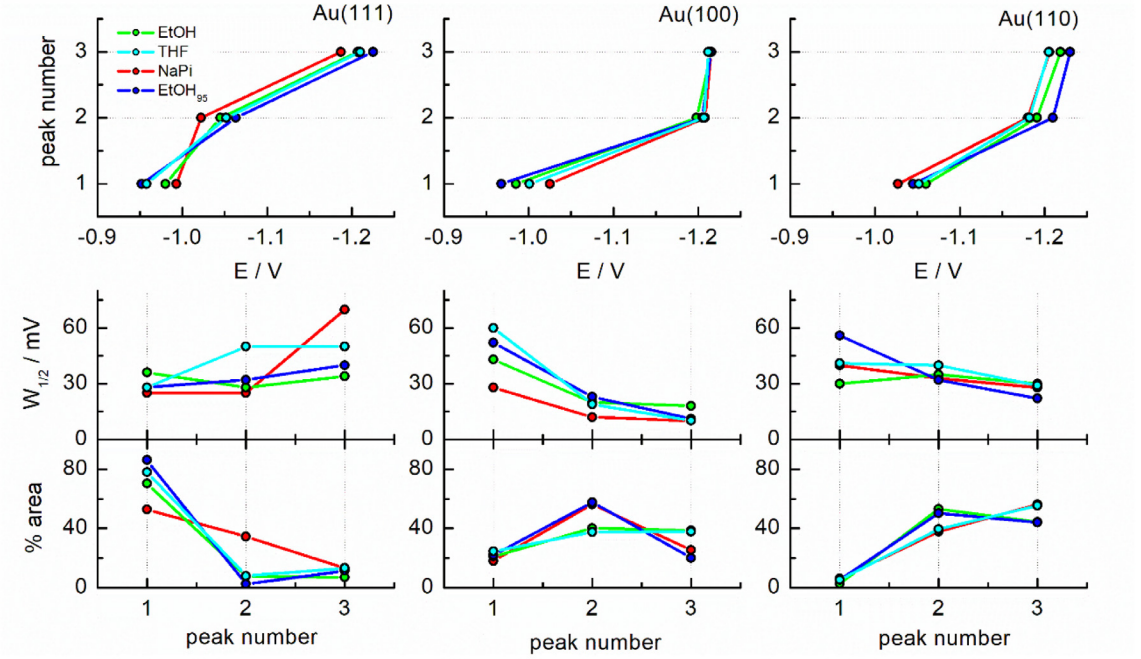

Fig. 4. Parameters obtained in the deconvolution of the cyclic voltammograms reductive desorption main peaks recorded in the Au(1 1 1), Au(1 0 0) and Au(1 1 0) single crystal electrodes. The potentials of the three contributions (peaks 1, 2 and 3 in decreasing potential order) are plotted in the top graphics. The lower panel gathers the half width and the percentage area of every deconvoluted peak for the three single crystal surfaces.

gle crystal electrodes [27,34,36,38,42], and the features have been assigned to the sequential desorption from sites with different binding energies [34,36], or monolayer domains with different sizes and stability [35], or depletion micelles that can be formed on the double layer region [33,36,47,48], and finally, they have been ascribed to the relative importance of the different intermolecular interactions that are present through the monolayer [49]. Thus, the deconvolution of the main peaks including two contributions should be explained as the presence of domains where the EG7 molecules are organized with different orientations that give place to intermolecular interactions of different magnitude. If we consider that the length of the EG7-SH chain can be longer than the hexadecanethiol, that gives place to multi-wave voltammetry at Au(1 1 1) single crystal gold electrodes [35], it is expected that, under some circumstances, the same behavior can be found in the EG7-SAM on the three single crystal faces studied in this work.

One interesting aspect of the EG7-SAMs formed on different single crystal facets is that the charge densities involved in the reductive desorption process are similar independent on the formation media but somewhat different for each facet, being of around 20% higher for Au(1 1 1) and Au(1 0 0), and 5% lower than that for the PO gold electrode (Table S1). By taking into account the surface atomic densities (1.39×10^{15}, 1.20×10^{15}, and 0.85×10^{15}, for the Au(1 1 1), (1 0 0) and (1 1 0) planes, respectively) [50], and the surfaces coverages determined from the charge densities, the coverages obtained are of 0.30, 0.33 and 0.39 for Au(1 1 1), Au(1 0 0) and Au(1 1 0), respectively.

Table 1
Water contact angles measured for the EG7-SAMs assembled in different modification solvents.

Modification solvent	Contact angle/$\Theta_{(H2O)}$
NaPi 1 M	53.3 ± 1.2
THF	48.2 ± 2.4
$EtOH_{95}$	61.0 ± 2.1
EtOH	71.3 ± 3.1

3.2. Contact angles measurements of the EG7-SAMs

The water contact angles of these EG7-SAMs have been measured and the results are gathered in Table 1. The highest values obtained for the SAMs formed in ethanolic solutions point to a higher exposure of the methyl groups to the interface. A lower value is measured for the EG7-SAM formed in NaPi that probably reflect the higher content of water on the topmost layer even though the experiment is made with a dried surface. The lowest value obtained for the SAM formed in THF can be related to the less organized structure that is presumed in this media in agreement with previous work [31], and that can allow the exposure of some EG units to the external surface creating a more hydrophilic environment.

3.3. Evaluation of the blocking behavior of the EG7-SAMs formed in different media

Another interesting point to check is the electrochemical response of these SAMs against the redox pair $[Fe(CN)_6]^{3-/4-}$. We choose this redox probe because recent works have shown that, while other systems as $[Ru(NH_3)_6]^{3+/2+}$, $Fc(MeOH)_2]^{+/0}$ and $[IrCl_6]^{2-/3-}$, maintain their reversible behavior and are not inhibited by the presence of the monolayer, the $[Fe(CN)_6]^{3-/4}$ electron transfer is completely suppressed at the EG7-SAM prepared in NaPi 1 M solution [27–29].

The experimental strategy used here is the preparation of the EG7-SAMs in the different media used in the above section (NaPi 1 M, EtOH, $EtOH_{95}$ and THF) and their evaluation by cyclic voltammetry and electrochemical impedance spectroscopy by using the $[Fe(CN)_6]^{3-/4}$ redox probe in three different solutions (c.a., NaPi 0.1 M at pH 7, KNO_3 0.1 M and KCl 0.1 M). As previously reported [28,29], the inhibition of the electron transfer signal is complete when the cyclic voltammogram of the EG7-SAM formed in 1 M NaPi is recorded in a NaPi 0.1 M solution (Fig. 5). A strong inhibition, although lower than the above, is also observed when the $[Fe(CN)_6]^{3-/4}$ redox pair is explored in either KNO_3 or KCl 0.1 M solutions. The Nyquist plots obtained under the same experimental conditions are also included in Fig. 5 and the results for the rest of experimental conditions are included in Figure S2, where the data are also represented as Bode plots to highlight the observed changes. The impedance data show the typical semicircles representing the charge transfer resistance with total absence of the Warburg element,

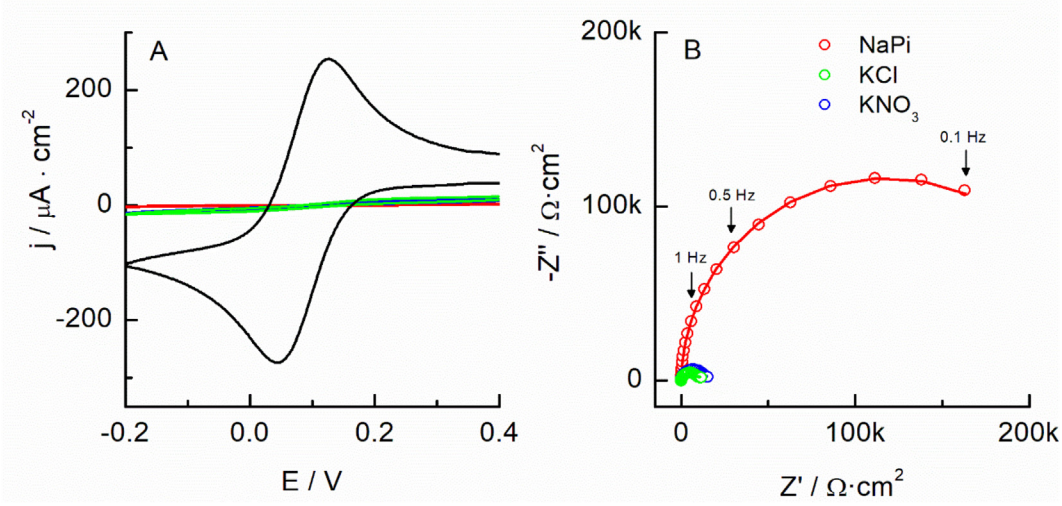

Fig. 5. (A) Cyclic voltammograms recorded at a scan rate of 0.1 V/s, and (B) impedance spectra of 1 mM $K_3Fe(CN)_6$ and 1 mM $K_4[Fe(CN)_6$ in 0.1 M electrolyte solutions (as indicated in the figure label) in the presence of EG7-SAMs formed in 1 M NaPi at pH 7.4. The black line corresponds to the curve recorded with the naked gold electrode.

indicating no diffusion contribution. The spectra have been fitted by using a Randles equivalent circuit (either with or without Warburg component) and the results are included in Table S1. The capacitor has been substituted by a constant phase element to improve the fitting and account for deviations from ideal capacitive behavior (CPE $= (Q(i\omega)^n)^{-1}$, where Q and n are the magnitude and exponent parameter of the CPE). We have used Eqn. (1) to calculate the effective capacitance,

$$C = \sqrt[n]{\frac{Q}{\left(R_s^{-1} + R_{CT}^{-1}\right)^{1-n}}} \quad (1)$$

where R_s and R_{CT} are the solution and the charge transfer resistance obtained from fitting the impedance spectra. The capacitance values are gathered in Table 2. Table 3 gathers the electron transfer rate constant values obtained by using Eqn. (2).

$$k_{ap} = \frac{RT}{n^2 \cdot F^2 \cdot R_{ct} \cdot A \cdot c} \quad (2)$$

where R is the gas constant, T the temperature, F the Faraday constant, n the number of electrons, A the geometric area of the electrode and c the concentration of the redox pair and R_{CT} the charge transfer resistance obtained in the fits (Table S1).

It can be seen that the as-prepared EG7-SAM blocks the $[Fe(CN)_6]^{3-/4}$ electron transfer similarly, and thus, the electron transfer rate constants are practically independent of the nature of the solvent employed in the formation solution. However, a strong dependence on the electrolyte used for the electrochemical evaluation is observed. Whereas the stronger inhibition is always obtained when the experiment is run in NaPi 0.1 M solutions, an increase in the electron transfer rate constant of an order of magnitude is observed when the redox probe is assayed in either KNO_3 or KCl solutions.

The peculiar blocking behavior of $[Fe(CN)_6]^{3-/4}$ redox probe that has been interpreted in terms of the hydration properties of both the monolayer and the electroactive anions [28], together with the classical view of the existence of repulsive interactions that affect the concentration profiles of the redox probe in the surrounding of the electron transfer active sites [51–54], can help in the understanding of this phenomenon.

In contrast to what has been observed for the reductive desorption processes, the inhibition of the electron transfer of the redox probe is not much influenced by the nature of the solvent employed in the formation of the EG7-SAM. Only little differences are obtained that, most of them, are within the experimental variability of these systems. We expected some influence of the presence of water in the formation solution but, probably, the small amount of these molecules that remains within the EG7 assembled chains is not reflected in the external face of the layer. Deeply investigations on this topic have evidenced that during EGn-SAM growth in aqueous solutions, and under conditions of high surface coverage, the increased binding of thiol molecules constitute a driving force for structural changes within the monolayer that press out the water molecules that are previously interacting with the EG groups. This effect is considered to occur at higher temperature but, under room temperature conditions as these used in our work, this driving force should not operate and the water molecules interacting with the EG moieties maintain these rather strong interactions [55]. In this respect, even assuming that compact monolayers are formed in the four solutions employed, the EG7-SAMs formed in $EtOH_{95}$ and NaPi solutions should contain certain water molecules within the chains. Moreover, although it has been found that once the monolayers are dried and newly immersed in water solutions, they are impermeable to water molecules [17], when they are examined by infrared spectroscopy under a water layer, some changes in the peak frequencies along with peak broadening are observed that are interpreted as penetration of some water molecules into the external monolayer region that result in the formation of hydrogen bonds with the oxygen atoms of the EG moieties [16,17,20,55,56]. The strong interaction between the EG units with water may then stablish a transition of structured aqueous layer at the film/liquid interface [21] independently of the fact that the SAMs were formed in aqueous solutions or not.

At this point, it is interesting to note the important effect of the electrolyte used for the electrochemical evaluation of the SAMs by the $[Fe(CN)_6]^{3-/4}$ redox probe. As the electrochemical measurement is made after equilibrating the modified electrode with the solution, there is plenty of time for the water molecules and the electrolyte ions to interact with the external region of the EG7-SAM. The slightly negative charge measured for EGn films [57,58] can allow the interaction with cations, in this case the Na^+ or K^+ ions, that exist in a high concentration in the electrolyte. To explore the existence of a long-range structured water layer adjacent to the EGn interface, Dicke et al. [59] made force-distance measurements under different electrolyte solutions. They employed both chaotropic and kosmotropic ions following the Hofmeister series to investigate their influence on water structure and the possible interaction with the EG units of the SAM, but they could not find a conclusive effect as all the ions studied showed a similar trend independent of their position in the series. The necessity of certain amount of space for a complexation between the EG units and the cations that should not be available in the densely packed SAM was used as the reason for the lack of effects.

However, the role of different ions in the formation of two-phase systems with EGn polymers is well documented and a different ability is found for Na^+ and K^+ and even for phosphate salts. These effects are explained on the basis of their position on the Hofmeister series and their free energy of hydration. Thus, the presence of these salts can decrease the amount of water available in the vicinity of the monolayer changing the structure of the interface [60]. If the structural changes in the external region of the EG7-SAM are dependent on the ability of the ions to make the layer more impermeable to the redox probe, the observed differences in the electron transfer rate constants of the $[Fe(CN)_6]^{3-/4}$ redox probe could be explained. To ascertain if this effect is produced by the Na^+ or the phosphate ions, apart from the studies in KNO_3 and KCl, we have also studied the influence of other salts like NaCl or KPi. Under these conditions, the same behavior is observed allowing us to conclude that is only the combination effect

Table 2
Double layer capacitance of the EG7-SAM, determined by using Eqn. (1), and the data obtained in the fitting of impedance spectra of EG7-SAM PO gold electrodes prepared in four different media and evaluated in 1 mM $[Fe(CN)_6]^{3-/4}$ in three electrolyte solutions.

$Cdl/\mu F \cdot cm^{-2}$	Evaluation media		
Formation media	NaPi	KNO_3	KCl
NaPi 1 M	3.9	4.2	4.3
THF	5.0	4.9	4.9
$EtOH_{95}$	4.1	5.0	5.0
EtOH	5.2	4.2	5.2

Table 3
Electron transfer rate constants (k_{ap}) of the $[Fe(CN)_6]^{3-/4}$ redox probe, determined by using Eqn. (2), and the R_{ct} data obtained in the fitting of impedance spectra of EG7-SAM PO gold electrodes prepared in four different media and evaluated in 1 mM $[Fe(CN)_6]^{3-/4}$ in three electrolyte solutions (Table S1).

k_{ap} $(x\ 10^6)/cm \cdot s^{-1}$	Evaluation media		
Formation media	NaPi	KNO_3	KCl
NaPi 1 M	0.5	9.3	13.4
THF	0.4	3.4	4.9
$EtOH_{95}$	0.9	2.4	2.6
EtOH	0.5	4.5	4.7

of Na^+ and phosphate ions that provoke the stronger inhibition of the $[Fe(CN)_6]^{3-/4}$ electron transfer.

To find out if after exposure of the EG7-SAMs to the electrolyte solutions, some ions can remain adhered to the external region of the monolayer, X-ray photoelectronic spectra have been recorded for EG7-SAMs that have been contacted overnight with each of the electrolyte solutions used in this work. In any of the cases, we could detect the presence of them as it has been the case reported in earlier studies dealing with the same propose [59]. Moreover, no changes in the composition and/or binding energies of the S 2p, C 1 s and O 1 s signals corresponding to the SAMs were detected that could allow some conclusions about the presence of those ions in the monolayer that could explain the observed behavior. Figure S3 shows the spectra obtained in high resolution for the S 2p, C 1 s and O 1 s, for the EG7-SAMs formed in $EtOH_{95}$ and NaPi 1 M, after being in contact overnight with the electrolyte solution. The S 2p spectra are dominated by the peak at 162 eV corresponding to the thiolate species bound to gold, as it was observed for the EG7-SAM formed in EtOH [27]. However, an increase in the ratio of free thiol or di-sulfur groups in the deconvoluted spectra is found in respect to the SAM formed in the absence of water (25–30 % in the present case, whereas less than 20 % of the area corresponding to the high energy peaks, in the case of EtOH). The spectra obtained for the C 1 s and O 1 s are deconvoluted with three components being the strongest peaks assigned to the carbon and oxygen atoms in the EG segments. The rest of components are ascribed to adventitious carbons or oxygen functions coming from impurities that are very difficult to eliminate. The presence of some water molecules that remains within the SAM (~532.5 eV [61]) cannot be discarded.

4. Conclusions

Compact EG7-SAMs can be formed from EtOH, $EtOH_{95}$, THF and NaPi 1 M aqueous solutions of EG7 on gold substrates as evidenced by the analysis of the reductive desorption processes. When using a PO gold electrode, subtle differences are observed in the shape and potentials of the various peaks that are ascribed to the different interactions of the solvent with the EG7 chains and the probable retention of some water molecules within the self-assembled chains. The formation of EG7-SAMs on low index gold single crystals allows us to assign the peaks to different facets of gold and speculate on the existence of possible interactions that give place to different organization depending on the size of the domains within the monolayer.

The differences observed in the reductive desorption processes of the EG7-SAMs formed in various solvents are not translated into the blocking behavior of these films as analyzed by cyclic voltammetry and electrochemical impedance spectroscopy of the $[Fe(CN)_6]^{3-/4}$ redox pair in different electrolytes. A stronger inhibition of the electron transfer of the probe is obtained in NaPi 0.1 M aqueous solution in comparison with the other electrolytes such as KNO_3, KCl, NaCl and KPi. There must be specific interactions between the Na^+ or phosphate or both ions that can change either the structure of the topmost region of the monolayer establishing specific interactions with the ether oxygens, or the structure of the water film directly interacting with the monolayer. However, no experimental evidence has been found for any of these possibilities, concluding that a repulsion effect for an increase of the negative charge in the monolayer that occurs in the presence of NaPi must be responsible for this stronger inhibition of the electron transfer. In this respect, a recent study investigating the breakdown of protein resistance in OEG-terminated alkanethiol SAMs [62], has proposed that trivalent ions replace the structured water molecules coupled in an interfacial water layer to the SAM, as a possible mechanism in overcoming the protein resistance.

CRediT authorship contribution statement

Miriam Chávez: Conceptualization, Methodology, Validation, Investigation. **Guadalupe Sánchez-Obrero:** Conceptualization, Methodology, Writing – review & editing. **Rafael Madueño:** Conceptualization, Methodology, Writing – review & editing. **José Manuel Sevilla:** Conceptualization, Methodology, Writing – review & editing. **Manuel Blázquez:** Conceptualization, Methodology, Writing – original draft, Writing – review & editing. **Teresa Pineda:** Conceptualization, Methodology, Writing – original draft, Writing – review & editing, Funding acquisition, Conceptualization, Methodology, Writing – original draft, Writing – review & editing, Funding acquisition.

Declaration of Competing Interest

The authors declare that they have no known competing financial interests or personal relationships that could have appeared to influence the work reported in this paper.

Acknowledgements

We thank the Ministerio de Ciencia e Innovación (Project RED2018-102412-T Network of Excellence Electrochemical Sensors and Biosensors), Junta de Andalucía and Universidad de Cordoba (UCO-FEDER-2018: ref. 1265074-2B and Plan Propio, Submod. 1.2. P.P. 2019) for financial support of this work. M.C. acknowledges Ministerio de Universidades for FPU 17/03873 grant. Funding for open access charge: Universidad de Córdoba / CBUA.

Appendix A. Supplementary data

Supplementary data to this article can be found online at https://doi.org/10.1016/j.jelechem.2022.116303.

References

[1] J.C. Love, L.A. Estroff, J.K. Kriebel, R.G. Nuzzo, G.M. Whitesides, Self-assembled monolayers of thiolates on metals as a form of nanotechnology, Chem. Rev. 105 (4) (2005) 1103–1169.
[2] A. Ulman, Formation and structure of self-assembled monolayers, Chem. Rev. 96 (4) (1996) 1533–1554.
[3] R. Yamada, H. Sakai, K. Uosaki, Solvent effect on the structure of the self-assembled monolayer of alkanethiol, Chem. Lett. 7 (1999) 667–668.
[4] T.W. Schneider, D.A. Buttry, Electrochemical quartz crystal microbalance studies of adsorption and desorption of self-assembled monolayers of alkyl thiols on gold, J. Am. Chem. Soc. 115 (26) (1993) 12391–12397.
[5] A.H.A. Mamun, J.R. Hahn, Effects of solvent on the formation of octanethiol self-assembled monolayers on Au(111) at High temperatures in a closed vessel: A scanning tunneling microscopy and X-ray photoelectron spectroscopy study, J. Phys. Chem. C 116 (42) (2012) 22441–22448.
[6] D. Yan, J.A. Saunders, G.K. Jennings, Enhanced chain densities of n-alkanethiolate self-assembled monolayers on gold from aqueous micellar solutions, Langmuir 16 (20) (2000) 7562–7565.
[7] D. Yan, J.A. Saunders, G.K. Jennings, Kinetics of formation for n-alkanethiolate self-assembled monolayers onto gold in aqueous micellar solutions of C12E6 and C12E7, Langmuir 18 (26) (2002) 10202–10212.
[8] D. Yan, J.A. Saunders, G.K. Jennings, Formation and stability of hexadecanethiolate SAMs prepared in aqueous micellar solutions of C12E6, Langmuir 19 (22) (2003) 9290–9296.
[9] V. Ganesh, V. Lakshminarayanan, Self-assembled monolayers of alkanethiols on gold prepared in a hexagonal lyotropic liquid crystalline phase of triton X-100/water system, Langmuir 22 (4) (2006) 1561–1570.
[10] D. García Raya, R. Madueno, M. Blazquez, T. Pineda, Formation of a 1,8-octanedithiol self-assembled monolayer on Au(111) prepared in a lyotropic liquid-crystalline medium, Langmuir 26 (14) (2010) 11790–11796.
[11] D. Garcia Raya, C. Silien, M. Blazquez, T. Pineda, R. Madueño, Electrochemical and AFM study of the 2D-assembly of colloidal gold nanoparticles on dithiol SAMs tuned by ionic strength, J. Phys. Chem. C 118 (26) (2014) 14617–14628.
[12] A.R. Puente Santiago, T. Pineda, M. Blazquez, R. Madueño, Formation of 2-D crystalline intermixed domains at the molecular level in binary self-assembled

monolayers from a lyotropic mixture, J. Phys. Chem. C 120 (16) (2016) 8595–8606.
[13] A.R. Puente Santiago, G. Sánchez-Obrero, T. Pineda, M. Blázquez, R. Madueño, Influence of patterning in the acid-base interfacial properties of homogeneously mixed CH3- and COOH-terminated self-assembled monolayers, J. Phys. Chem. C 122 (5) (2018) 2854–2865.
[14] S. Herrwerth, W. Eck, S. Reinhardt, M. Grunze, Factors that determine the protein resistance of oligoether self-assembled monolayers - Internal hydrophilicity, terminal hydrophilicity, and lateral packing density, J. Am. Chem. Soc. 125 (31) (2003) 9359–9366.
[15] P. Harder, M. Grunze, R. Dahint, G.M. Whitesides, P.E. Laibinis, Molecular conformation in oligo(ethylene glycol)-terminated self-assembled monolayers on gold and silver surfaces determines their ability to resist protein adsorption, J. Phys. Chem. B 102 (2) (1998) 426–436.
[16] M.W.A. Skoda, R.M.J. Jacobs, J. Willis, F. Schreiber, Hydration of oligo(ethylene glycol) self-assembled monolayers studied using polarization modulation infrared spectroscopy, Langmuir 23 (3) (2007) 970–974.
[17] S. Zorn, N. Martin, A. Gerlach, F. Schreiber, Real-time PMIRRAS studies of in situ growth of C(11)Eg(6)OMe on gold and immersion effects, Phys. Chem. Chem. Phys. 12 (31) (2010) 8986–8991.
[18] L.Y. Li, S.F. Chen, J. Zheng, B.D. Ratner, S.Y. Jiang, Protein adsorption on oligo (ethylene glycol)-terminated alkanethiolate self-assembled monolayers: The molecular basis for nonfouling behavior, J. Phys. Chem. B 109 (7) (2005) 2934–2941.
[19] K.L. Prime, G.M. Whitesides, Adsorption of proteins onto surfaces containing end-attached oligo(ethylene oxide) - A model system using self-assembled monolayers, J. Am. Chem. Soc. 115 (23) (1993) 10714–10721.
[20] M.W.A. Skoda, F. Schreiber, R.A.J. Jacobs, J.R.P. Webster, M. Wolff, R. Dahint, D. Schwendel, M. Grunze, Protein density profile at the interface of water with oligo (ethylene glycol) self-assembled monolayers, Langmuir 25 (7) (2009) 4056–4064.
[21] R.L.C. Wang, H.J. Kreuzer, M. Grunze, Molecular conformation and solvation of oligo(ethylene glycol)-terminated self-assembled monolayers and their resistance to protein adsorption, J. Phys. Chem. B 101 (47) (1997) 9767–9773.
[22] R.L.C. Wang, H.J. Kreuzer, M. Grunze, The interaction of oligo(ethylene oxide) with water: a quantum mechanical study, Phys. Chem. Chem. Phys. 2 (16) (2000) 3613–3622.
[23] M. Chavez, A. Fernandez-Merino, G. Sanchez-Obrero, R. Madueno, J.M. Sevilla, M. Blazquez, T. Pineda, Distinct thermoresponsive behaviour of oligo- and poly-ethylene glycol protected gold nanoparticles in concentrated salt solutions, Nanoscale Adv. 3 (16) (2021) 4767–4779.
[24] G. Emilsson, R.L. Schoch, L. Feuz, F. Höök, R.Y.H. Lim, A.B. Dahlin, Strongly stretched protein resistant poly(ethylene glycol) brushes prepared by grafting-to, ACS Appl. Mater. Interfaces 7 (14) (2015) 7505–7515.
[25] R. Ortiz, S. Olsen, E. Thormann, Salt-induced control of the grafting density in poly (ethylene glycol) brush layers by a grafting-to approach, Langmuir 34 (15) (2018) 4455–4464.
[26] G. Sanchez-Obrero, M. Chavez, R. Madueno, M. Blazquez, T. Pineda, J.M. Lopez-Romero, F. Sarabia, J. Hierrezuelo, R. Contreras-Caceres, Study of the self-assembly process of an oligo(ethylene glycol)-thioacetyl substituted theophylline (THEO) on gold substrates, J. Electroanal. Chem. 823 (2018) 663–671.
[27] M. Chávez, G. Sánchez-Obrero, R. Madueño, J.M. Sevilla, M. Blázquez, T. Pineda, Characterization of a self-assembled monolayer of O-(2-Mercaptoethyl)-O′-methyl-hexa(ethylene glycol) (EG7-SAM) on gold electrodes, J. Electroanal. Chem. 880 (2021) 114892.
[28] T. Doneux, A. de Ghellinck, E. Triffaux, N. Brouette, M. Sferrazza, C. Buess-Herman, Electron transfer across an antifouling mercapto-hepta(ethylene glycol) self-assembled monolayer, J. Phys. Chem. C 120 (29) (2016) 15915–15922.
[29] T. Doneux, L. Yahia Cherif, C. Buess-Herman, Controlled tuning of the ferri/ferrocyanide electron transfer at oligo(ethylene glycol)-modified electrodes, Electrochim. Acta 219 (2016) 412–417.
[30] A.L. Gui, E. Luais, J.R. Peterson, J.J. Gooding, Zwitterionic phenyl layers: finally, stable, anti-biofouling coatings that do not passivate electrodes, ACS Appl. Mater. Interfaces 5 (11) (2013) 4827–4835.
[31] D.J. Vanderah, G. Valincius, C.W. Meuse, Self-assembled monolayers of methyl 1-thiahexa(ethylene oxide) for the inhibition of protein adsorption, Langmuir 18 (12) (2002) 4674–4680.
[32] C.A. Widrig, C. Chung, M.D. Porter, The electrochemical desorption of n-alkanethiol monolayers from polycrystalline gold and silver electrodes, J. Electroanal. Chem. 310 (1–2) (1991) 335–359.
[33] C.J. Zhong, J. Zak, M.D. Porter, Voltammetric reductive desorption characteristics of alkanethiolate monolayers at single crystal Au(111) and (110) electrode surfaces, J. Electroanal. Chem. 421 (1–2) (1997) 9–13.
[34] M.M. Walczak, C.A. Alves, B.D. Lamp, M.D. Porter, Electrochemical and X-ray photoelectron spectroscopic evidence for differences in the binding sites of alkanethiolate monolayers chemisorbed at gold, J. Electroanal. Chem. 396 (1–2) (1995) 103–114.
[35] C.J. Zhong, M.D. Porter, Fine structure in the voltammetric desorption curves of alkanethiolate monolayers chemisorbed at gold, J. Electroanal. Chem. 425 (1–2) (1997) 147–153.
[36] S.S. Wong, M.D. Porter, Origin of the multiple voltammetric desorption waves of long-chain alkanethiolate monolayers chemisorbed on annealed gold electrodes, J. Electroanal. Chem. 485 (2) (2000) 135–143.
[37] D.F. Yang, C.P. Wilde, M. Morin, Electrochemical desorption and adsorption of nonyl mercaptan at gold single crystal electrode surfaces, Langmuir 12 (26) (1996) 6570–6577.
[38] T. Doneux, M. Steichen, A. De Rache, C. Buess-Herman, Influence of the crystallographic orientation on the reductive desorption of self-assembled monolayers on gold electrodes, J. Electroanal. Chem. 649 (1–2) (2010) 164–170.
[39] T. Laredo, J. Leitch, M. Chen, I.J. Burgess, J.R. Dutcher, J. Lipkowski, Measurement of the charge number per adsorbed molecule and packing densities of self-assembled long-chain monolayers of thiols, Langmuir 23 (11) (2007) 6205–6211.
[40] O. Azzaroni, M.E. Vela, G. Andreasen, P. Carro, R.C. Salvarezza, Electrodesorption potentials of self-assembled alkanethiolate monolayers on Ag(111) and Au(111). An electrochemical, scanning tunneling microscopy and density functional theory study, J. Phys. Chem. B 106 (47) (2002) 12267–12273.
[41] N. Arisnabarreta, G.D. Ruano, M. Lingenfelder, E.M. Patrito, F.P. Cometto, Comparative study of the adsorption of thiols and selenols on Au(111) and Au (100), Langmuir 33 (48) (2017) 13733–13739.
[42] R. Madueno, J.M. Sevilla, T. Pineda, A.J. Roman, M. Blazquez, A voltammetric study of 6-mercaptopurine monolayers on polycrystalline gold electrodes, J. Electroanal. Chem. 506 (2) (2001) 92–98.
[43] S. Yoshimoto, T. Sawaguchi, F. Mizutani, I. Taniguchi, STM and voltammetric studies on the structure of a 4-pyridinethiolate monolayer chemisorbed on Au (100)-(1 × 1) surface, Electrochem. Commun. 2 (1) (2000) 39–43.
[44] K. Arihara, T. Ariga, N. Takashima, T. Okajima, F. Kitamura, K. Tokuda, T. Ohsaka, Multiple voltammetric waves for reductive desorption of cysteine and 4-mercaptobenzoic acid monolayers self-assembled on gold substrates, Phys. Chem. Chem. Phys. 5 (17) (2003) 3758–3761.
[45] D. Grumelli, L.J. Cristina, F.L. Maza, P. Carro, J. Ferrón, K. Kern, R.C. Salvarezza, Thiol adsorption on the Au(100)-hex and Au(100)-(1 × 1) Surfaces, J. Phys. Chem. C 119 (25) (2015) 14248–14254.
[46] F.P. Cometto, Z. Luo, S. Zhao, J.A. Olmos-Asar, M.M. Mariscal, Q. Ong, K. Kern, F. Stellacci, M. Lingenfelder, The van der Waals interactions of n-alkanethiol-covered surfaces: from planar to curved surfaces, Angew. Chem. Int. Ed. 56 (52) (2017) 16526–16530.
[47] M. Byloos, H. Al-Maznai, M. Morin, Formation of a self-assembled monolayer via the electrospreading of physisorbed micelles of thiolates, J. Phys. Chem. B 103 (31) (1999) 6554–6561.
[48] D.F. Yang, H. AlMaznai, M. Morin, Vibrational study of the fast reductive and the slow oxidative desorptions of a nonanethiol self-assembled monolayer from a Au (111) single crystal electrode, J. Phys. Chem. B 101 (7) (1997) 1158–1166.
[49] I. Thom, M. Buck, On the interpretation of multiple waves in cyclic voltammograms of self-assembled monolayers of n-alkane thiols on gold, Z. Phys. Chem. 222 (5–6) (2008) 739–754.
[50] X. Gao, G.J. Edens, F.-C. Liu, M.J. Weaver, A. Hamelin, Sensitivity of electrochemical adlayer structure to the metal crystallographic orientation: potential-dependent iodide adsorption on Au(100) in comparison with other low-index surfaces, J. Phys. Chem. 98 (33) (1994) 8086–8095.
[51] K. Takehara, H. Takemura, Y. Ide, Electrochemical studies of the terminally substituted alkanethiol monolayers formed on a gold electrode - effects of the terminal group on the redox responses of Fe(Cn)6-N-3-, Ru(Nh3)H-6-3+ and ferrocenedimethanol, Electrochim. Acta 39 (6) (1994) 817–822.
[52] T.H. Degefa, P. Schon, D. Bongard, L. Walder, Elucidation of the electron transfer mechanism of marker ions at SAMs with charged head groups, J. Electroanal. Chem. 574 (1) (2004) 49–62.
[53] J.M. Campina, A. Martins, F. Silva, Selective permeation of a liquidlike self-assembled monolayer of 11-amino-1-undecanethiol on polycrystalline gold by highly charged electroactive probes, J. Phys. Chem. C 111 (14) (2007) 5351–5362.
[54] R. Madueno, D. Garcia-Raya, A.J. Viudez, J.M. Sevilla, T. Pineda, M. Blazquez, Influence of the solution pH in the 6-mercaptopurine self-assembled monolayer (6MP-SAM) on a Au(111) single-crystal electrode, Langmuir 23 (22) (2007) 11027–11033.
[55] S. Zorn, M.W.A. Skoda, A. Gerlach, R.M.J. Jacobs, F. Schreiber, On the stability of oligo(ethylene glycol) (C11EG6OMe) SAMs on gold: behavior at elevated temperature in contact with water, Langmuir 27 (6) (2011) 2237–2243.
[56] M. Zolk, F. Eisert, J. Pipper, S. Herrwerth, W. Eck, M. Buck, M. Grunze, Solvation of oligo(ethylene glycol)-terminated self-assembled monolayers studied by vibrational sum frequency spectroscopy, Langmuir 16 (14) (2000) 5849–5852.
[57] H.J. Kreuzer, R.L.C. Wang, M. Grunze, Hydroxide ion adsorption on self-assembled monolayers, J. Am. Chem. Soc. 125 (27) (2003) 8384–8389.
[58] C. Dicke, G. Hähner, pH-dependent force spectroscopy of tri(ethylene glycol)- and methyl-terminated self-assembled monolayers adsorbed on gold, J. Am. Chem. Soc. 124 (42) (2002) 12619–12625.
[59] C. Dicke, G. Hähner, Interaction between a Hydrophobic Probe and Tri(ethylene glycol)-Containing Self-assembled Monolayers on Gold Studied with Force Spectroscopy in Aqueous Electrolyte Solution, J. Phys. Chem. B 106 (17) (2002) 4450–4456.
[60] S.C. Silvério, O. Rodríguez, J.A. Teixeira, E.A. Macedo, The effect of salts on the liquid-liquid phase equilibria of PEG600 + salt aqueous two-phase systems, J. Chem. Eng. Data 58 (12) (2013) 3528–3535.
[61] X.-P. He, X.-W. Wang, X.-P. Jin, H. Zhou, X.-X. Shi, G.-R. Chen, Y.-T. Long, Epimeric monosaccharide−quinone hybrids on gold electrodes toward the electrochemical probing of specific carbohydrate−protein recognitions, J. Am. Chem. Soc. 133 (10) (2011) 3649–3657.
[62] M.W.A. Skoda, N.F. Conzelmann, M.R. Fries, L.F. Reichart, R.M.J. Jacobs, F. Zhang, F. Schreiber, Switchable β-lactoglobulin (BLG) adsorption on protein resistant oligo (ethylene glycol) (OEG) self-assembled monolayers (SAMs), J. Colloid Interface Sci. 606 (2022) 1673–1683.